Impact of Mission Profile Dynamics on Accuracy of Thermal Stress Modeling in PV Inverters

Sangwongwanich, Ariya; Wang, Huai; Blaabjerg, Frede

Published in:
Proceeding of 2020 IEEE Energy Conversion Congress and Exposition (ECCE)

DOI (link to publication from Publisher):
10.1109/ECCE44975.2020.9235750

Publication date:
2020

Document Version
Early version, also known as pre-print

Impact of Mission Profile Dynamics on Accuracy of Thermal Stress Modeling in PV Inverters

Ariya Sangwongwanich, Huai Wang, and Frede Blaabjerg
Department of Energy Technology, Aalborg University, Aalborg, Denmark
ars@et.aau.dk, hwa@et.aau.dk, fbl@et.aau.dk

***Abstract*—Thermal stress modeling of power devices is a key factor that influences the design for reliability of Photovoltaic (PV) inverters under long-term operations, i.e., different mission profiles. Due to the requirement of long-term analysis for mapping the inverter reliability more accurately, a thermal model based on a lumped thermal network is normally employed due to its low computational burden. However, there is still a lack of validation in terms of modeling accuracy, e.g., comparing the simulation results against the experimental thermal stress in field operations. Besides, the impact of mission profile dynamics on the accuracy of different thermal modeling approaches have not been analyzed. To address this issue, the model accuracy of two thermal stress modeling approaches for PV inverters are evaluated in this paper by comparing the thermal stress estimated from a thermal model with the experimental results under various mission profile dynamics. According to the results, the average error of the junction temperature estimation is 1.51 % for a transient thermal model and 2.08 % for a steady-state thermal model, respectively. On the other hand, the computational efficiency of the thermal stress modeling can be improved by more than a factor of three when using the steady-state thermal model.**

***Index Terms*—Insulated-gate bipolar transistor (IGBT), thermal modeling, reliability, mission profile, Photovoltaic (PV) systems, inverters.**

I. Introduction

Thermal stress is a key factor that influences the reliability of PV inverters [1]–[3]. Power devices such as Insulated-Gate Bipolar Transistors (IGBTs) are among the reliability-critical components in the PV inverters, which are subjected to high thermal stress during the inverter operation [4]. Accordingly, thermal stress modeling of the power devices is essential to ensure reliable operation of PV inverters, especially under long-term operating conditions, which will wear-out the components [5]. In that case, the mission profile, which is a representation of the inverter operating condition, needs to be considered during the thermal stress analysis [6]. In PV applications, the mission profile consists of the solar irradiance and ambient temperature, which has a time-span of several days to months when considering a seasonal variation of the mission profile dynamics. Therefore, a long-term thermal stress analysis is generally demanded for PV applications, which brings a significant challenge to the thermal modeling of the power device.

Several thermal models have been developed for power electronics applications, especially for the power devices, ranging from a very simplified one (e.g., based on a lumped thermal network) to a highly complex one (e.g., based on a finite-element model) [7]–[14]. In general, there is usually a trade-off between complexity and accuracy of different thermal modeling approaches. However, due to the requirement of long-term simulation studies, a lumped thermal network is typically applied for analyzing thermal stress under mission profile operation due to its low computational burden and simple parameterization [15]–[22]. In previous studies, the lumped thermal network is either based on the transient thermal model [15]–[19], which includes all the transient thermal impedance, or the steady-state lumped thermal model [20]–[22], which only considers the thermal resistance. While this thermal stress modeling approach has been widely accepted in the previous studies, to the best knowledge of the authors, there is still a lack of validation in terms of modeling accuracy, especially when comparing the simulation results against the experimental thermal stress in field operations.

Besides, the impact of mission profile dynamics on the accuracy of different thermal modeling approaches for PV inverters have not been analyzed in the previous studies. In fact, by knowing the dynamics of the mission profile, a suitable thermal model can be employed, which further simplifies the thermal modeling process. This technique has been applied for power converters in Wind Turbine (WT) applications [23], [24], where different lumped-thermal models have been used for different time-scales of the mission profile dynamics. It was concluded in [23] that the transient thermal model with a relatively high-detailed lumped thermal network is required for the seconds-minutes range mission profile dynamics, while the steady-state thermal model should be employed only when the mission profile dynamic is in the range of a few hours.

However, the same conclusion cannot be directly applied to the thermal stress analysis of PV inverters, mainly due to the different dynamics of the cooling system. In WT power converters, the water-cooled heatsink is normally used, which results in a fast thermal response of the case (and also heatsink) temperature [23], [25]. Therefore, most of the thermal stress dynamics occur within the junction and case of the power device module. In contrast, most of the PV inverters employ an air-cooled heatsink [3], which has a much longer time-constant of the thermal impedance. Consequently, most of the thermal stress dynamics in the PV inverter is actually induced by the case temperature variation, while the temperature between the junction and case of the power device module can reach steady-state much faster. Accordingly, different approaches for selecting the thermal model should be applied for the

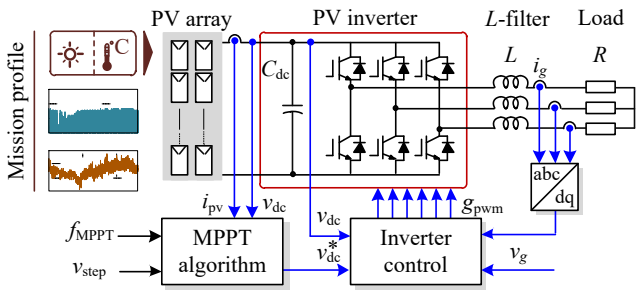

Fig. 1. System diagram and control structure of PV inverter test-bench with maximum power point tracking (MPPT) control strategy implemented.

TABLE I
PARAMETERS OF THE THREE-PHASE PV INVERTER TEST-BENCH.

PV array rated power	2500 W
Output current (rated)	i_g = 30 A
DC-link voltage	v_{dc} = 400-600 V
DC-link capacitance	C_{dc} = 340 μF
Filter inductance	L = 2.5 mH
Resistive load	R = 16.5 Ω
Switching frequency	f_{sw} = 10 kHz
Nominal output frequency	f_g = 50 Hz
Ambient temperature	T_a = 25 °C

thermal stress modeling of PV inverters, where the time-constant of the power device thermal impedance (and also the cooling system) and the mission profile dynamics need to be considered together. Moreover, the computational efficiency is another aspect that also needs to be considered when selecting the thermal modeling approach, especially for a long-term simulation condition, e.g., mission profile. These aspects have not been addressed in the previous research, and a guideline for selecting a suitable thermal modeling approach has not been discussed so far.

In this paper, the thermal stress modeling approaches for PV inverter are analyzed, where the mission profile dynamics are taken into consideration. The experimental measurement of the thermal stress from the PV inverter test-bench is carried out in Section II and used as a benchmark. In Section III, two thermal modeling approaches based on a lumped thermal network, namely, the steady-state and the transient thermal models, are discussed. Various mission profile dynamics are applied to the thermal models, and their model accuracy and computational efficiency are evaluated in Section IV. Finally, concluding remarks are provided in Section V.

II. IMPACT OF MISSION PROFILE DYNAMICS

A. Test-Bench of PV Inverter

In this work, a test-bench for PV inverter, which allows an experimental measurement of power device junction temperature during mission profile operation, has been developed following the overall system diagram in Fig. 1 and the system parameters in Table I. A 1200V/50A three-phase IGBT module from [26], which is shown in Fig. 2, is used as the power stage.

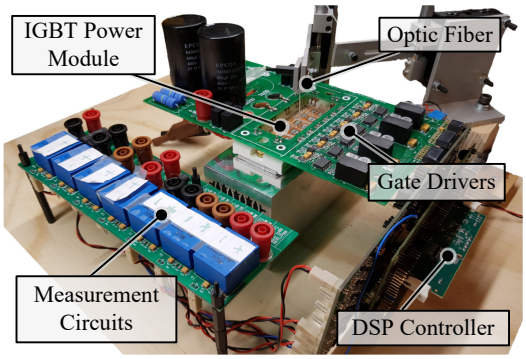

Fig. 2. Hardware prototype of the PV inverter test-bench where the IGBT junction temperature is measured by using an optic fiber.

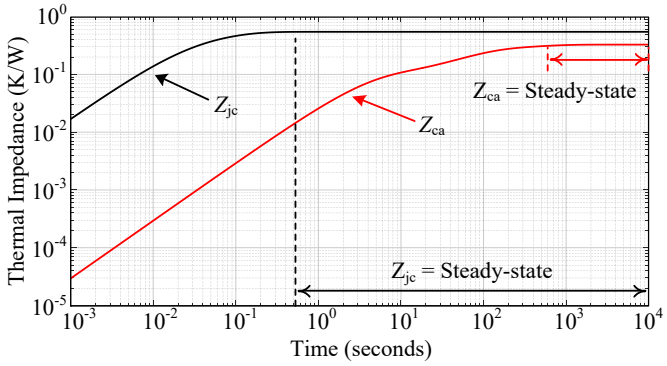

Fig. 3. Thermal impedance characteristic of the IGBT module between junction and case Z_{jc} as well as case and ambient Z_{ca} [26].

TABLE II
PARAMETERS OF THE THERMAL IMPEDANCE NETWORK BETWEEN JUNCTION AND CASE OF THE IGBT MODULE Z_{JC} [26].

Layer i	1	2	3	4
Thermal resistance $R_{jc,i}$	0.0324	0.1782	0.1728	0.1566
Thermal capacitance $C_{jc,i}$	0.3086	0.1122	0.2894	0.6386

TABLE III
PARAMETERS OF THE THERMAL IMPEDANCE NETWORK BETWEEN CASE OF THE IGBT MODULE AND AMBIENT CONDITION Z_{CA}.

Layer i	1	2	3
Thermal resistance $R_{ca,i}$	0.0670	0.1737	0.0869
Thermal capacitance $C_{ca,i}$	6,157	404.72	37.335

The thermal impedance characteristics of the IGBT module and the cooling system are shown in Fig. 3. The parameters of the thermal impedance network between junction and case Z_{jc} and between the case and ambient Z_{ca} are summarized in Tables II and III, respectively. It can be seen from the hardware prototype that the Printed Circuit Board (PCB) is custom-made, which allows for direct access to the IGBT chip, and the junction temperature can be directly measured through an optic fiber, e.g., under real-field mission profile operation.

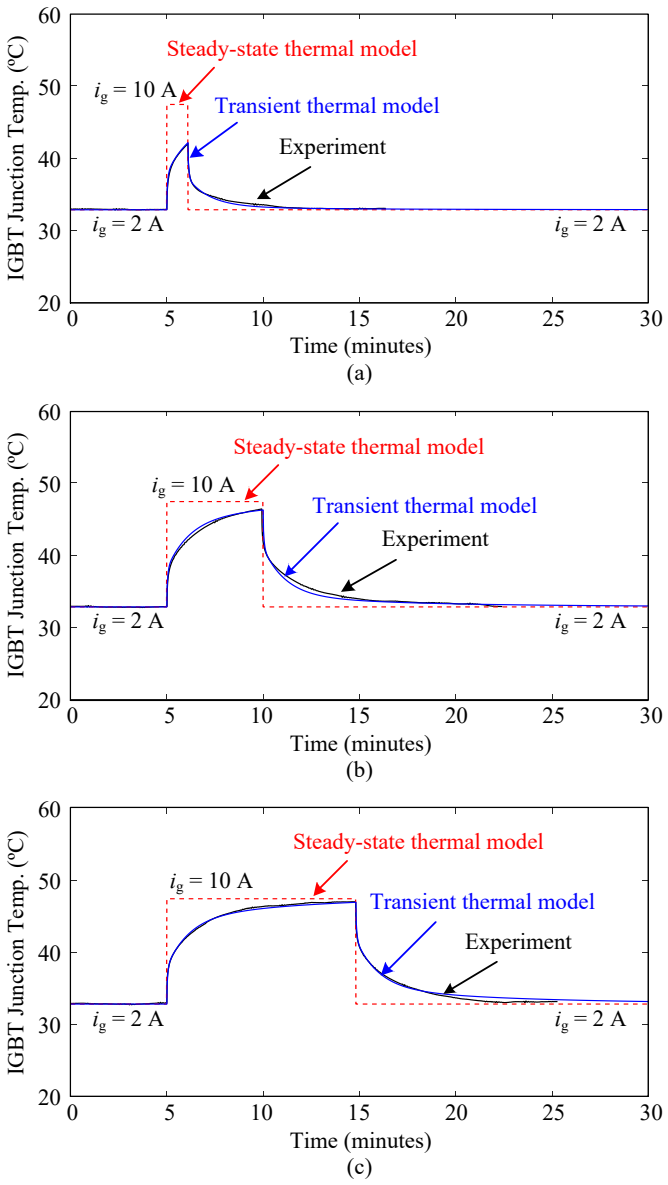

Fig. 4. Simulation and experimental results of thermal stress obtained from the transient and steady-state thermal models when the load dynamics (i.e., load durations) are: a) 1 minute, b) 5 minutes, and c) 10 minutes.

B. Impact of Load Dynamics on the Thermal Stress

According to the thermal impedance characteristics in Fig. 3, the thermal stress response is strongly dependent on the load (e.g., power losses) dynamics. In this case, the thermal impedance time-constant of the inverter is about 10 minutes (i.e., 600 seconds), which is dictated by the thermal impedance between the case and ambient Z_{ca}. This implies that if the load duration is longer than 10 minutes, the thermal stress of the IGBT (i.e., junction temperature T_j) will already reach the steady-state. On the contrary, the change in the junction temperature will be in the transient stage when the load duration is below 10 minutes due to the transient thermal impedance characteristic of the IGBT module.

The impact of load dynamics is demonstrated by applying the load durations of 1 minute, 5 minutes, and 10 minutes to the PV inverter test-bench. It can be seen from the experimental results in Fig. 4 that the final junction temperature is still in the transient state when the time duration of the load dynamics is 1 minute and 5 minutes. In contrast, when applying the load duration of 10 minutes to the test-bench, the final junction temperature of the IGBT is reaching the steady-state. In fact, the final junction temperature of the case with 10-minutes load duration is about 5.3 °C higher than in the case with 1-minute load duration. This indicates a significant impact of the load dynamics and the time-constant of the thermal impedance on the thermal stress modeling.

C. Impact of Mission Profile Dynamics on the Thermal Stress

In PV applications, the load duration of the inverter in real-field operation is dictated by the mission profile dynamics. In practice, the long-term mission profile is recorded with a certain sampling rate, referred to as a resolution of the mission profile. To demonstrate the impact of mission profile dynamics on the thermal stress variation in real-field operation, the mission profiles with the resolutions of 1 second, 1 minute, 5 minutes, and 10 minutes, which are recorded from the same day, are applied to the PV inverter test-bench. The obtained thermal stress profiles are shown in Fig. 5, where the thermal stress obtained from the mission profile with a resolution of 1 second per sample is used as a benchmark case (representing the most accurate mission profile dynamics). It can be seen from the results in Fig. 5(a) that most of the thermal stress dynamics can still be captured when applying a 1-minute resolution mission profile. However, when the mission profile resolution reduces further to 10 minutes, which is shown in Fig. 5(c), the fast variation in the thermal stress is no longer represented, and the maximum junction temperature estimation deviates significantly from the case with 1-second mission profile resolution. The absence of fast variation in the thermal stress due to a low resolution of the mission profile will influence the choice of the thermal modeling approach.

III. Thermal Stress Modeling of PV Inverters

In this section, two conventional thermal modeling approaches based on a lumped thermal network will be presented. The advantages and limitations of each thermal model in thermal stress modeling will be discussed.

A. Transient Thermal Model

The most commonly used approach for thermal stress modeling has previously been presented in Fig. 6 [15]–[19]. This model will be referred to as a transient thermal model, since it includes all transient thermal impedances in the thermal network (e.g., between the junction and case Z_{jc} and between the case and ambient Z_{ca}). The presence of the thermal capacitance makes this thermal model capable of representing the dynamics of the thermal stress behavior accurately. However, it also increases the computational burden, especially when

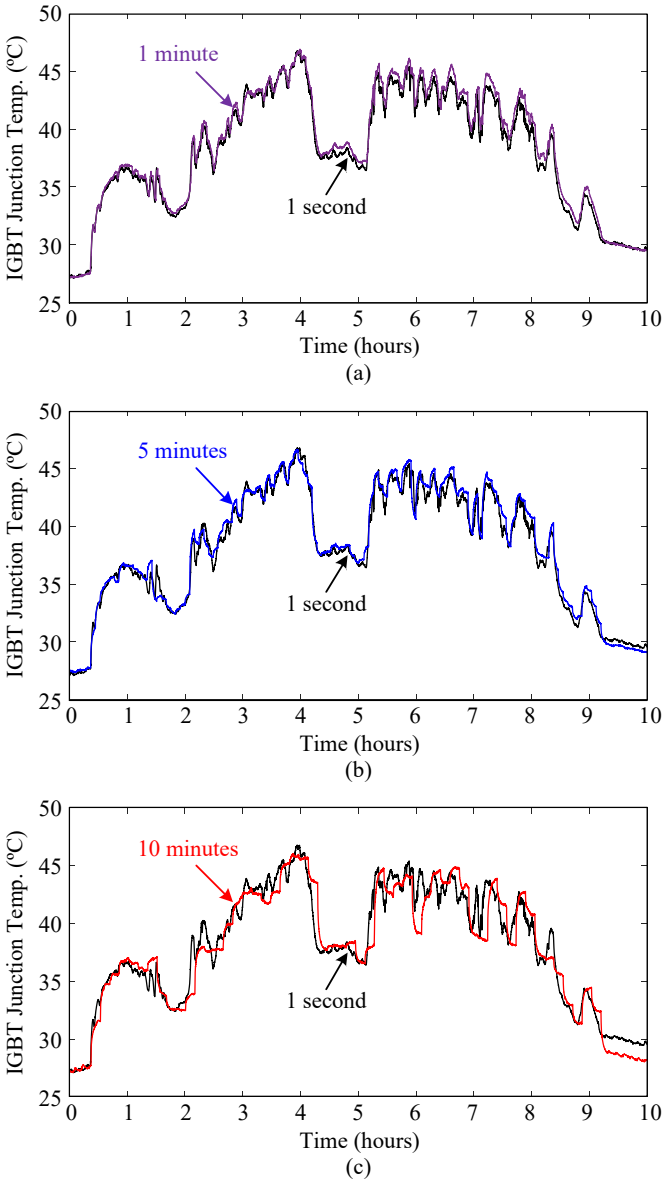

Fig. 5. Experimental results of the thermal stress of the PV inverter under one-day mission profile with the resolutions of: a) 1 minute, b) 5 minutes, and c) 10 minutes, where the 1-second mission profile is used as a reference.

the number of order increases, which is the main drawback of this thermal modeling method.

A comparison between the experimental and simulation results with a transient thermal model is carried out by applying a step-load at different load durations. According to the results in Fig. 4, the transient thermal model can capture the dynamics of the thermal stress well regardless of the load duration. It can also be noticed that the final junction temperature is not reaching the steady-state when the load duration of 1 minute and 5 minutes are applied as shown in Fig. 4(a) and 4(b). This demonstrates the case where the load dynamics are below the time-constant of the thermal impedance Z_{ca}, which is about 10 minutes according to Fig. 3.

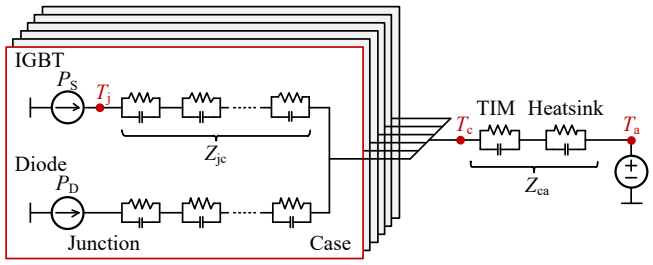

Fig. 6. Thermal model of three-phase IGBT module in PV inverter based on transient lumped thermal network (TIM: Thermal Interface Material).

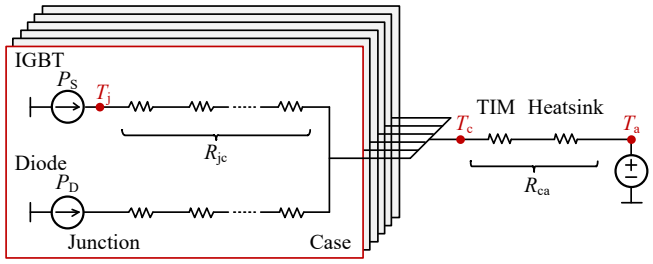

Fig. 7. Thermal model of three-phase IGBT module in PV inverter based on steady-state lumped thermal network (TIM: Thermal Interface Material).

B. Steady-State Thermal Model

Another thermal modeling approach, which is commonly used for long-term thermal stress analysis, is the steady-state thermal model [20]–[22]. In this approach, the thermal network is represented only by the thermal resistance, as shown in Fig. 7, while the thermal capacitance, which mainly influences the transient dynamics, is neglected. On one hand, this thermal model is very straightforward and resource-effective in terms of implementation and computation. It also provides a good accuracy of the thermal stress estimation during steady-state. On the other hand, the transient behavior of the thermal stress cannot be captured with this steady-state thermal model, since there is no time-constant of the thermal impedance, due to the absence of the thermal capacitance.

The thermal stress profiles obtained from the steady-state thermal model under different load durations are also shown in Fig. 4. It can be seen from the results in Fig. 4(a) and 4(b) that there is a certain deviation in the thermal stress estimation, e.g., maximum junction temperature, when the load duration is below 10 minutes, which is the time-constant of the thermal impedance Z_{ca}. However, the steady-state model can estimate the junction temperature (e.g., final value) quite accurately when the load duration is above the time-constant of the thermal impedance Z_{ca} (which is closer to the steady-state), as it is shown in Fig. 4(c).

IV. Benchmarking of Thermal Stress Modeling

In this section, a one-day mission profile with the resolutions of 1 second, 1 minute, 5 minutes, and 10 minutes are applied to the transient and steady-state thermal models. The

thermal stress modeling accuracy is evaluated by comparing the estimated thermal stress from simulations with the experimental results obtained from the PV inverter test-bench (under the same mission profile resolution).

A. Thermal Stress Analysis

The simulation and experimental results of the thermal stress when applying the transient thermal model are shown in Fig. 8. Since all the transient thermal impedances are considered in the transient thermal model, the dynamics of the thermal stress can be estimated accurately even during the fast variation as it is shown in Fig. 8(a). At the same time, the thermal stress under a slow variation of the mission profile dynamics in Fig. 8(d) can also be accurately estimated.

The same mission profiles are also applied to the steady-state thermal model as it is shown in Fig. 9. It can be seen that the steady-state thermal model introduces a considerable error in the thermal stress estimation when the mission profile resolution is 1 second. This confirms that the assumption of a steady-state thermal impedance modeling is no longer valid when the load duration is below the time-constant of the thermal impedance. On the other hand, the steady-state thermal model can effectively estimate the thermal stress of the PV inverter when the load duration is 10 minutes, which is above the time-constant of the thermal impedance, as it is shown in Fig. 9(d). In that case, the difference between the thermal estimation from the transient and steady-state thermal models becomes less significant, since the thermal stress is mostly in steady-state.

B. Model Accuracy

The accuracy of the thermal stress modeling can be evaluated from the average deviation of the junction temperature estimation. In this case, the average deviation ε between the junction temperature profile obtained from the simulation $T_{\text{j,sim}}$ and the experiment $T_{\text{j,exp}}$ (under the same mission profile resolution) can be calculated as:

$$\varepsilon = \frac{|T_{\text{j,exp}} - T_{\text{j,sim}}|}{T_{\text{j,exp}}} \cdot 100 \qquad (1)$$

The average deviation of the junction temperature estimation when applying the different thermal models under various mission profile resolutions is summarized in Table IV. In general, it can be seen that the estimation deviation decreases as the mission profile resolution decreases, which is similar to the observation in the time-domain waveforms of the thermal stress profiles. On the other hand, the accuracy of the thermal stress estimation can be improved by employing the transient thermal models, where the deviation from the two models are comparable. For all mission profile resolutions that are being considered, the maximum average deviation for the junction temperature estimation is 2.08 %, which is the case when applying a 1-second mission profile resolution to the steady-state thermal model.

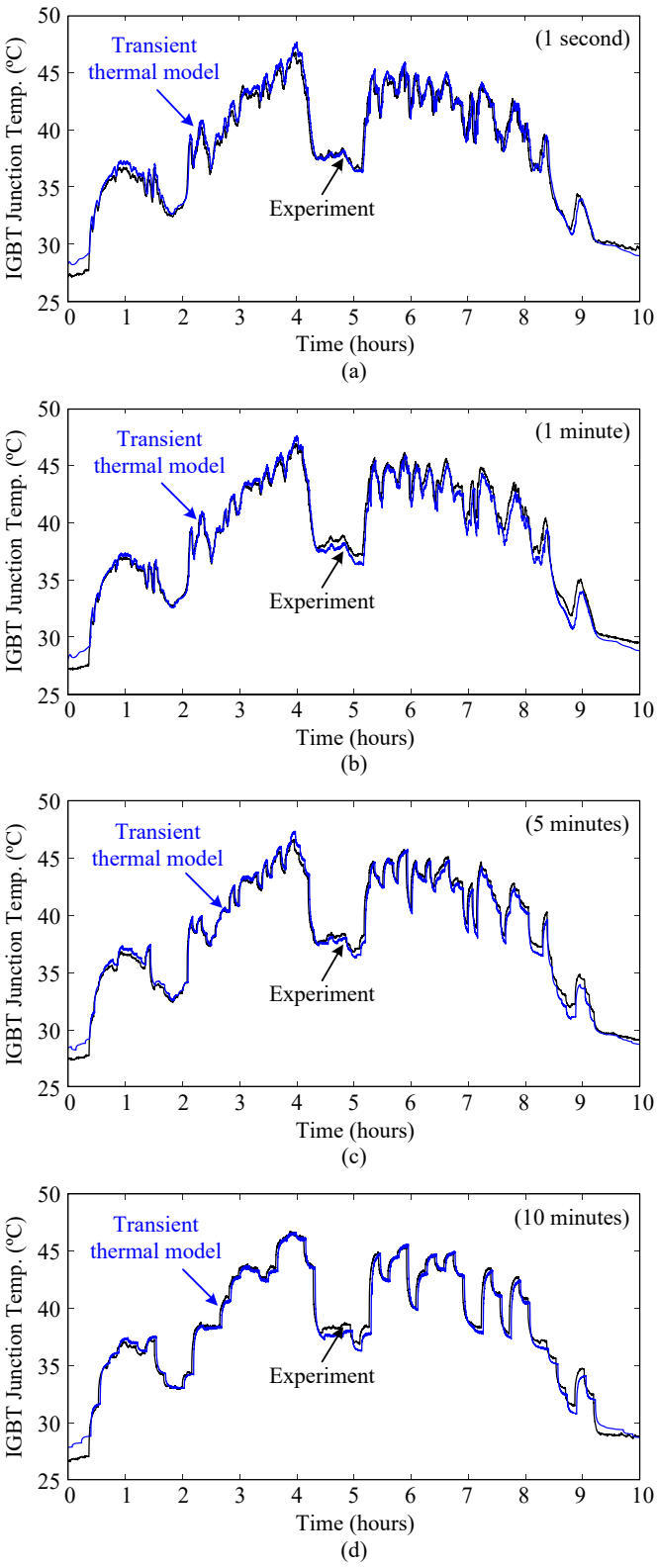

Fig. 8. Simulation and experimental results of thermal stress obtained from the transient thermal model when the one-day mission profile with the resolutions of: a) 1 second, b) 1 minute, c) 5 minutes, and d) 10 minutes, are applied, where the ambient temperature is T_{a} = 25 °C.

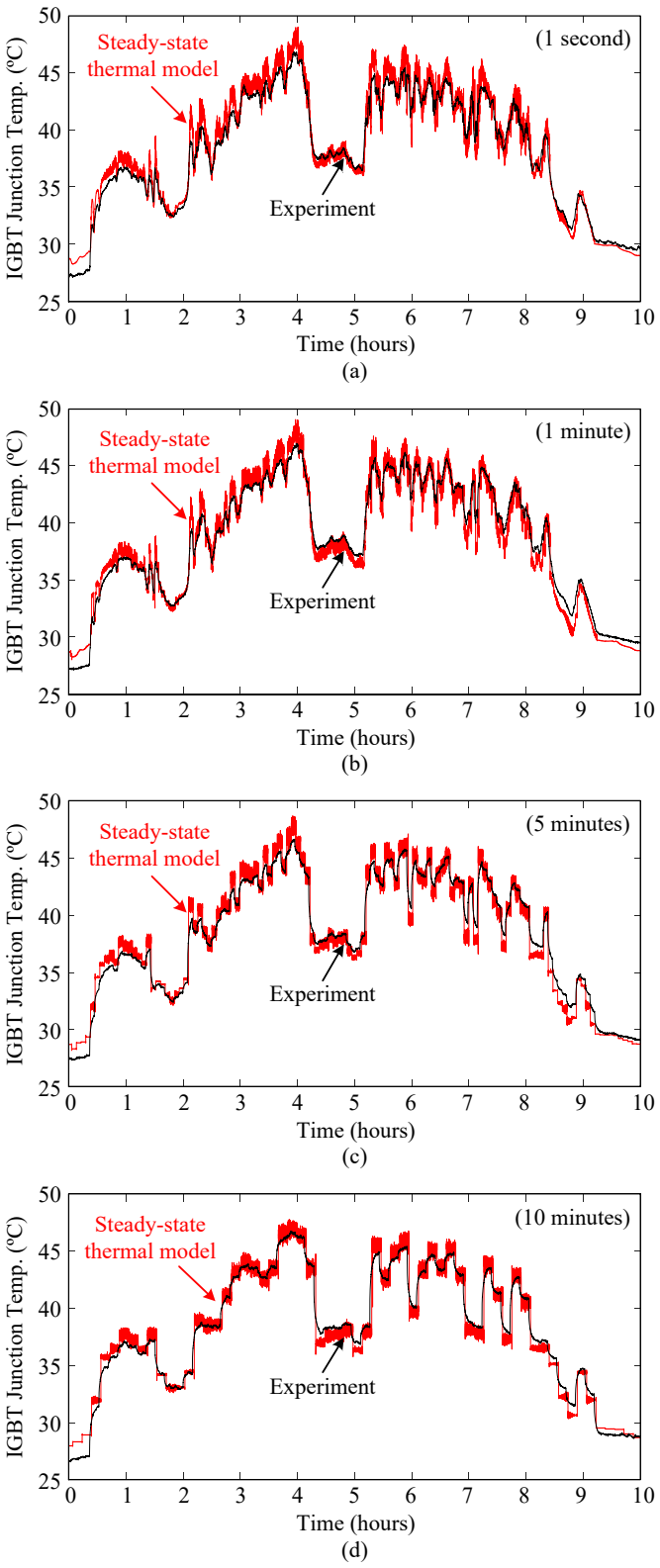

Fig. 9. Simulation and experimental results of thermal stress obtained from the steady-state thermal model when the one-day mission profile with the resolutions of: a) 1 second, b) 1 minute, c) 5 minutes, and d) 10 minutes, are applied, where the ambient temperature is T_a = 25 °C.

TABLE IV
AVERAGE DEVIATION BETWEEN SIMULATION AND EXPERIMENTAL RESULTS OF THERMAL STRESS ε (FROM FIGS. 8 AND 9).

Mission Profile Resolution	Transient Thermal Model	Steady-State Thermal Model
1 second	1.50 %	2.08 %
1 minute	1.51 %	2.03 %
5 minutes	1.33 %	1.94 %
10 minutes	0.83 %	1.78 %

TABLE V
REQUIRED SIMULATION TIME OF THERMAL MODELS FOR ONE-DAY THERMAL STRESS ANALYSIS.

Required Simulation Time	Transient Thermal Model	Steady-State Thermal Model
Mean μ	2.487 s	0.770 s
Standard Deviation σ	0.316 s	0.095 s

C. Computational Efficiency

Computational efficiency is another important aspect for thermal model selection, especially when considering a long-term analysis. To evaluate this aspect, the required simulation times for different thermal models have been measured when applying a one-day mission profile. The simulation of each thermal modeling approach has been repeated multiple times (e.g., 1000 times) in order to obtain a statistical value of the computational efficiency. The results are summarized in Table V, where it can be seen that the steady-state thermal model requires a much shorter simulation time compared to the transient thermal models. In fact, the required simulation time of the transient thermal model is three times longer than that of the steady-state model. This high computational burden is mainly introduced by a large number of RC elements in the lumped thermal model. Therefore, there is a trade-off between the model accuracy and computational efficiency when selecting the thermal modeling approach. The transient thermal model should be used when the fast dynamics of the thermal stress needs to be fully captured, e.g., when the mission profile resolution or load duration is below 10 minutes.

V. CONCLUSIONS

In this paper, the impact of mission profile dynamics on the accuracy of long-term thermal stress modeling has been analyzed for the power devices in PV inverters. Two thermal modeling approaches based on the lumped thermal network have been considered: 1) transient thermal model and 2) steady-state thermal model. The model accuracy has been evaluated by comparing the estimated thermal stress with the experimental results from the PV inverter test-bench, where various mission profile dynamics have been applied. According to the results, the steady-state thermal model has introduced a considerable error (i.e., 2.08 %) when a fast variation is applied in the mission profile dynamics. In contrast, the transient thermal model can provide a more accurate thermal

stress estimation at the expense of a higher computational burden, where the error is 1.51 %. These results provided validation in terms of thermal stress modeling accuracy of different thermal modeling approaches. A trade-off between the model accuracy and the computational efficiency for both the transient and steady-state thermal models is also given as a guideline for selecting the suitable thermal modeling approach according to thermal impedance characteristics and mission profile dynamics.

ACKNOWLEDGMENT

This work was supported in part by Innovation Fund Denmark through the Advanced Power Electronic Technology and Tools (APETT) project and in part by the Reliable Power Electronic-Based Power System (REPEPS) project at the Department of Energy Technology, Aalborg University as a part of the Villum Investigator Program funded by the Villum Foundation.

REFERENCES

[1] P. Hacke, S. Lokanath, P. Williams, A. Vasan, P. Sochor, G. TamizhMani, H. Shinohara, and S. Kurtz, "A status review of photovoltaic power conversion equipment reliability, safety, and quality assurance protocols," *Renew. Sustain. Energy Rev.*, vol. 82, pp. 1097–1112, 2018.

[2] Enphase Energy. Reliability - Enphase Energy. Online. [Online]. Available: https://enphase.com/en-au/enphase-advantage/reliability

[3] SMA, "Sunny boy/sunny tripower temperature derating." [Online]. Available: https://files.sma.de/dl/7418/Temp-Derating-TI-en-15.pdf

[4] N. R. Sorensen, E. V. Thomas, M. A. Quintana, S. Barkaszi, A. Rosenthal, Z. Zhang, and S. Kurtz, "Thermal study of inverter components," *IEEE J. Photovolt.*, vol. 3, no. 2, pp. 807–813, Apr. 2013.

[5] H. Wang, M. Liserre, and F. Blaabjerg, "Toward reliable power electronics: Challenges, design tools, and opportunities," *IEEE Ind. Electron. Mag.*, vol. 7, no. 2, pp. 17–26, Jun. 2013.

[6] M. Musallam, C. Yin, C. Bailey, and M. Johnson, "Mission profile-based reliability design and real-time life consumption estimation in power electronics," *IEEE Trans. Power Electron.*, vol. 30, no. 5, pp. 2601–2613, May 2015.

[7] V. Blasko, R. Lukaszewski, and R. Sladky, "On line thermal model and thermal management strategy of a three phase voltage source inverter," in *Proc. of IEEE IAS Annual Meeting*, vol. 2, pp. 1423–1431, Oct. 1999.

[8] Chan-Su Yun, P. Malberti, M. Ciappa, and W. Fichtner, "Thermal component model for electrothermal analysis of IGBT module systems," *IEEE Trans. Adv. Packag.*, vol. 24, no. 3, pp. 401–406, Aug. 2001.

[9] Z. Luo, H. Ahn, and M. A. E. Nokali, "A thermal model for insulated gate bipolar transistor module," *IEEE Trans. Power Electron.*, vol. 19, no. 4, pp. 902–907, Jul. 2004.

[10] M. Musallam and C. M. Johnson, "Real-time compact thermal models for health management of power electronics," *IEEE Trans. Power Electron.*, vol. 25, no. 6, pp. 1416–1425, Jun. 2010.

[11] B. Du, J. L. Hudgins, E. Santi, A. T. Bryant, P. R. Palmer, and H. A. Mantooth, "Transient electrothermal simulation of power semiconductor devices," *IEEE Trans. Power Electron.*, vol. 25, no. 1, pp. 237–248, Jan. 2010.

[12] C. Batard, N. Ginot, and J. Antonios, "Lumped dynamic electrothermal model of IGBT module of inverters," *IEEE Trans. Compon. Packag. Manuf. Technol*, vol. 5, no. 3, pp. 355–364, Mar. 2015.

[13] K. Ma, A. S. Bahman, S. Beczkowski, and F. Blaabjerg, "Complete loss and thermal model of power semiconductors including device rating information," *IEEE Trans. Power Electron.*, vol. 30, no. 5, pp. 2556–2569, May 2015.

[14] C. H. van der Broeck, L. A. Ruppert, A. Hinz, M. Conrad, and R. W. De Doncker, "Spatial electro-thermal modeling and simulation of power electronic modules," *IEEE Trans. Ind. App.*, vol. 54, no. 1, pp. 404–415, Jan. 2018.

[15] N. Sintamarean, H. Wang, F. Blaabjerg, and P. P. Rimmen, "A design tool to study the impact of mission-profile on the reliability of SiC-based PV-inverter devices," *Microelectron. Reliab.*, vol. 54, no. 9, pp. 1655 – 1660, 2014.

[16] P. D. Reigosa, H. Wang, Y. Yang, and F. Blaabjerg, "Prediction of bond wire fatigue of IGBTs in a PV inverter under a long-term operation," *IEEE Trans. Power Electron.*, vol. 31, no. 10, pp. 7171–7182, Oct. 2016.

[17] C. Felgemacher, S. Araujo, C. Noeding, P. Zacharias, A. Ehrlich, and M. Schidleja, "Evaluation of cycling stress imposed on IGBT modules in PV central inverters in sunbelt regions," in *Proc. of CIPS*, pp. 1–6, Mar. 2016.

[18] A. Sangwongwanich, Y. Yang, D. Sera, and F. Blaabjerg, "Lifetime evaluation of grid-connected PV inverters considering panel degradation rates and installation sites," *IEEE Trans. Power Electron.*, vol. 33, no. 2, pp. 1225–2361, Feb. 2018.

[19] R. K. Gatla, W. Chen, G. Zhu, J. V. Wang, and S. S. Kshatri, "Lifetime comparison of IGBT modules in grid-connected multilevel PV inverters considering mission profile," in *Proc. of. ICPE 2019 - ECCE Asia*, pp. 2764–2769, May 2019.

[20] S. E. De León-Aldaco, H. Calleja, F. Chan, and H. R. Jiménez-Grajales, "Effect of the mission profile on the reliability of a power converter aimed at photovoltaic applications - a case study," *IEEE Trans. Power Electron.*, vol. 28, no. 6, pp. 2998–3007, Jun. 2013.

[21] F. Chan and H. Calleja, "Reliability estimation of three single-phase topologies in grid-connected PV systems," *IEEE Trans. Ind. Electron.*, vol. 58, no. 7, pp. 2683–2689, Jul. 2011.

[22] E. Koutroulis and F. Blaabjerg, "Design optimization of transformerless grid-connected PV inverters including reliability," *IEEE Trans. Power Electron.*, vol. 28, no. 1, pp. 325–335, Jan. 2013.

[23] K. Ma, M. Liserre, F. Blaabjerg, and T. Kerekes, "Thermal loading and lifetime estimation for power device considering mission profiles in wind power converter," *IEEE Trans. Power Electron.*, vol. 30, no. 2, pp. 590–602, Feb. 2015.

[24] K. Ma and F. Blaabjerg, "Multi-timescale modelling for the loading behaviours of power electronics converter," in *Proc. of. ECCE*, pp. 5749–5756, Sep. 2015.

[25] *Transient thermal measurements and thermal equivalent circuit models*, Infineon Technologies AG, 2018, rev. 1.1.

[26] *FS50R12KT4_B15*, Infineon Technologies AG, 2009, rev. 3.0.